International Journal of Automotive Technology, Vol. 3, No. 4, pp. 157–163 (2002)

1229-9138/2002/004-04

ULTRASONIC DETECTION OF INTERFACE CRACK IN ADHESIVELY BONDED DCB JOINTS

N.-Y. CHUNG[1], S.-I. PARK[1]*, M.-D. LEE[2] and C.-H. PARK[3]

[1]Department of Mechanical Engineering, Soongsil University, Seoul 156-743, Korea
[2]Department of Mechanical Design Engineering, Dong Seoul College, Sungnam 461-714, Korea
[3]Hyundai Mechanical Institute, Seoul 150-033, Korea

(Received 22 May 2002; Revised 14 August 2002)

ABSTRACT–It is well recognized that the ultrasonic method is one of the most common and reliable nondestructive testing (NDT) methods for the quantitative estimation of defects in welded structures. However, NDT techniques applying for adhesively bonded joints have not been clearly established yet. In this paper, the detection of interface crack by the ultrasonic method was applied for the measurement of interfacial crack length in the adhesively bonded joints of double-cantilever beam (DCB). An optimal condition of transmission coefficients and experimental accuracy by the ultrasonic method in the adhesively bonded joints have been investigated and discussed. The experimental values are in good agreement with the computed results by boundary element method (BEM) and Ripling's equation.

KEY WORDS : Adhesively bonded joint, Double-cantilever beam, Interface crack, Ultrasonic method, Straight beam test, Angle beam test, Transmission coefficient, Boundary element method

1. INTRODUCTION

Recently the applications of adhesively bonded structures are rapidly increasing in the many industrial fields such as automobiles, aircrafts, ships and so on. Adhesive structures have various advantages compared with the mechanical fastened joints and the welded joints. The ultrasonic method is one of the most common and reliable nondestructive testing (NDT) methods for the quantitative estimation of defects in welded structures. When the ultrasonic method is applied to the interfacial crack detection for the adhesively bonded joints, the measuring error increases because of the spreading beam and scattering signal which is caused by the effects of thin thickness of adhesive layer and difference of material properties in dissimilar materials (Kline, 1987; Derouiche, 1995).

The initial crack often occurs on the bonded interface and it is the general cause of the interface fracture. It is very significant to establish the detection method of flaws by applying the ultrasonic technology into the interface cracks of adhesively bonded structures. However, ultrasonic testing techniques applying for adhesively bonded joints (Kline, 1986) clearly established yet.

In this paper, the interfacial crack lengths of adhesively bonded double-cantilever beam (DCB) joints were measured by the ultrasonic method. The accuracy of the crack lengths which were taken from the compliances by the experiment, the numerical analysis by the boundary element method (BEM) and Ripling's equation (Ripling, 1964; Chung, 2001) were investigated. As comparing them, the optimal ultrasonic conditions to improve the accuracy of interfacial crack detection by ultrasonic method are discussed and the systematic detection method of interface crack is proposed (Chung, 2001; Adler, 1972).

*Corresponding author. e-mail: sungilndt@hotmail.com

2. DETERMINATION OF TRANSMISSION COEFFICIENT

The equation of transmission coefficient of sound pressure from the straight beam test for the thickness variation of adhesive layer on the DCB specimen is given as follows (Koike, 1990):

$$t=\frac{1}{\sqrt{\cos^2 kh+\frac{1}{4}\left(\frac{Z_1}{Z_2}+\frac{Z_2}{Z_1}\right)^2\sin^2 kh}} \tag{1}$$

where h is thickness of adhesive layer and Z_i are impedances of materials respectively. Then $k=2\pi/\lambda$, $\lambda=C/f$, f is frequency, C is velocity of material and λ is wavelength.

Relationships between the sound velocity for adherend and the transmission coefficient of sound pressure for the angle of incidence, and refraction are given as follows (Moriyama, 1998):

$$t=\frac{C_{2s}\cdot C_{1L}}{C_{1s}^2}\cdot\frac{\cos\theta}{\cos\alpha}\cdot\frac{2(b^2-1)}{B} \tag{2}$$

where

$$a=\sqrt{(C/C_{2L})^2-1},\quad a'=\sqrt{(C/C_{1L})^2-1}$$

$$b=\sqrt{(C/C_{2S})^2-1},\quad b'=\sqrt{(C/C_{1S})^2-1}$$

$$B=\left[\frac{(b^2-1)}{2a}+2b\right]+\frac{\rho_2}{\rho_1}\left(\frac{C_{2S}}{C_{1S}}\right)^4\left[\frac{(b^2-1)^2}{2a}+2b'\right]$$

$$C=C_{2L}/\sin\alpha$$

C_{iL} and C_{iS} are ultrasonic velocities of longitudinal and shear wave for adherend respectively, and ρ_i are densities. Then α is incident angle and θ is refraction angle.

Table 1 shows the type of adhesively bonded DCB specimen. Type 1 and Type 2 are bonded homogeneous acryl and aluminum plates, respectively as adherends with cemedine 1500 (Ced. 1500) adhesive.

Table 2 and Table 3 list the material properties about the DCB specimens of Type 1 and Type 2.

Figure 1 indicates the transmission coefficient of sound pressure versus adhesive thickness from the material combination. The specimen of Type 1 was used to examine the interfacial crack length with optical microscope and its transmission coefficient of sound

Table 1. Type of adhesively bonded DCB specimen

Specimen	Adherend		Adhesive
	1	2	
Type 1	Acryl	Acryl	Ced. 1500
Type 2	Aluminum	Aluminum	

Table 2. Ultrasonic properties of adherend and adhesive

Specimen materials \ Material properties		Impedance, Z (10^6 kg/m^{2}s)	Longitudinal wave, C_L (m/s)
			Shear wave, C_S(m/s)
Adherend	Acryl	3.2	2,720
			1,460
	Aluminum	16.9	6,260
			3,080
Adhesive	Ced. 1500	2.2	2,034
			831

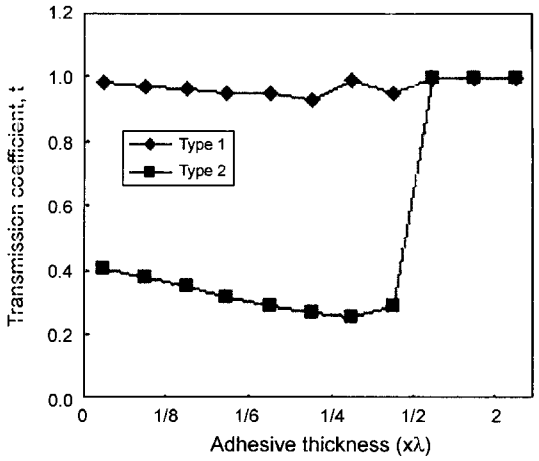

Figure 1. Transmission coefficient of adhesively bonded DCB specimen.

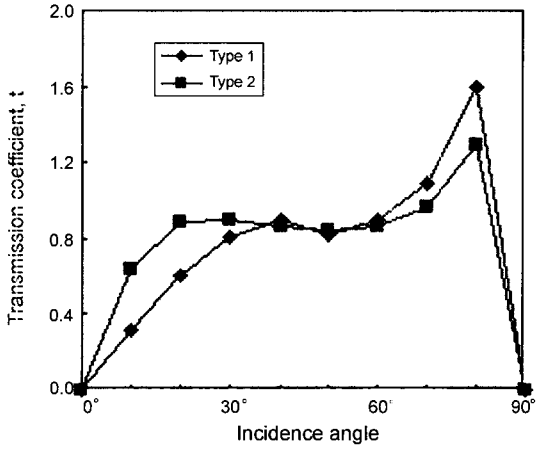

Figure 2. Transmission coefficient of adhesively bonded DCB specimen.

Table 3. Materials properties of adherend and adhesive

Specimen materials \ Material properties		Density ρ (10^3 kg/m^3)	Young's modulus E (GPa)	Poisson's ratio ν
Adherend	Acryl	1.18	2.94	0.35
	Aluminum	2.70	65.56	0.32
Adhesive	Ced.1500	1.07	2.06	0.40

pressure presents the stable and constant value. The specimen of Type 2 shows the rapid increase for the transmission coefficient of sound pressure at the range of $h > \lambda/3$.

Figure 2 shows the calculated results of the transmission coefficient of sound pressure about the incidence angle for the DCB specimens of Type 1 and Type 2. The transmission coefficient of sound pressure for the Type 1 and Type 2 greatly changes at the range of 20°~30° and 60°~80°, respectively. Thus, those two ranges are very useful optimal conditions for the angle beam test of ultrasonic methods.

3. EXPERIMENTAL

3.1. Specimen Configuration and Preparation

Adhesively bonded DCB specimen as shown in Figure 3, was employed in the present study. The adherends of Type 1 and Type 2 are the aluminum alloy and the acryl plate, respectively. Then, as adhesive the Cemedine 1500 was used and the initial crack was introduced with the teflon film of 0.2 mm thickness equal to adhesive layer.

In order to observe the interfacial crack length visually, the specimen of Type 2 was prepared with the acryl plate.

3.2. Experimental Method

The universal testing machine (Model 4206) was used and the load velocity was 0.5 mm/min under the constant displacement control in this experiment. The displacement of load point versus the interfacial crack length of the each specimen was drawn with X-Y recorder. The interfacial crack length was measured with the optical microscope and the ultrasonic tester (USK-7D) for the specimen of Type 1.

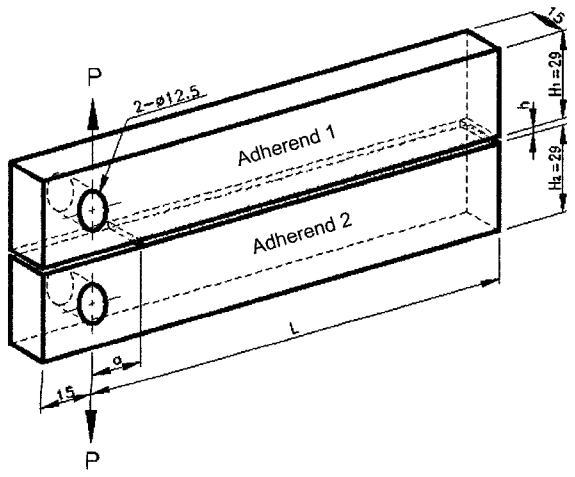

Figure 3. Shape and dimension of DCB joints.

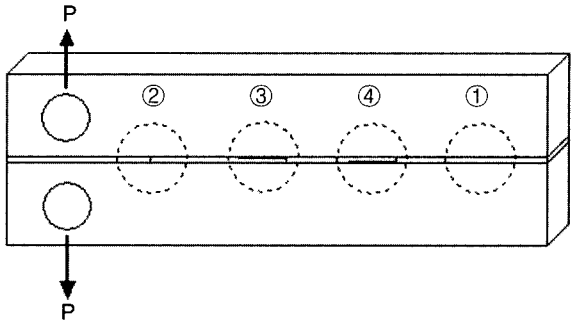

Figure 4. Schematic diagram of ultrasonic test.

The probe diameters of 5 mm and 10 mm, were used and its frequency was 4 MHz and 5 MHz, respectively in the straight beam test. For the angle beam test, the beam distance was kept within 0.5~1 skip distance. In the both cases of the straight and angle beam tests, interfacial crack length was detected by the 6 dB drop method.

In this experiment, the straight beam test was carried out within the thickness of adhesive layer $\lambda/3 < h < 2\lambda$ as shown Figure 1, and the angle beam test was measured within the incidence angle, 20°~30° and 60°~80°, as shown in Figure 2.

3.3. Measurement Accuracy of Interfacial Crack

We inserted teflon film in the Type 2 test specimen and formed an artificial crack. We compared differences between the echoes that were based on the sound pressure transmission coefficient results for each straight and angle beam test by the 6 dB drop ultrasonic method as shown in Figure 4.

In addition, this depicts the interface crack creating at the adhesive layer as the load is applied. Figure 5 shows the adhesive interface without any cracks as shown at the position ① of Figure 4. In case of the straight beam test as sown in Figure 5(a), the sound which reflects off the adhesive layer after it passed through the adherend 1, and the ultrasonic echo which reflects or returns off the base plane of the adherend 2 appear with a constant interval beam length. Ultrasonic echoes reflecting and returning on the adherend 1 and 2, are superposed on the inner part of adhesive layer. When the angle beam test is used as shown in Figure 5(b), the echo fails to pass the adhesive layer at 0.5-skip distance from the incidence point, thus it reflects and returns off the surface of the adherend 1 at 1.0-skip distance.

Figure 6 as shown at position ② of Figure 4, shows the ultrasonic echo that was measured in the straight and angle beam tests on the upper artificial interface crack-tip inserted with teflon film. In case of the straight beam test as shown in Figure 6(a), ultrasonic echo is separated after it passed through the adherend 1 and artificial crack-tip of

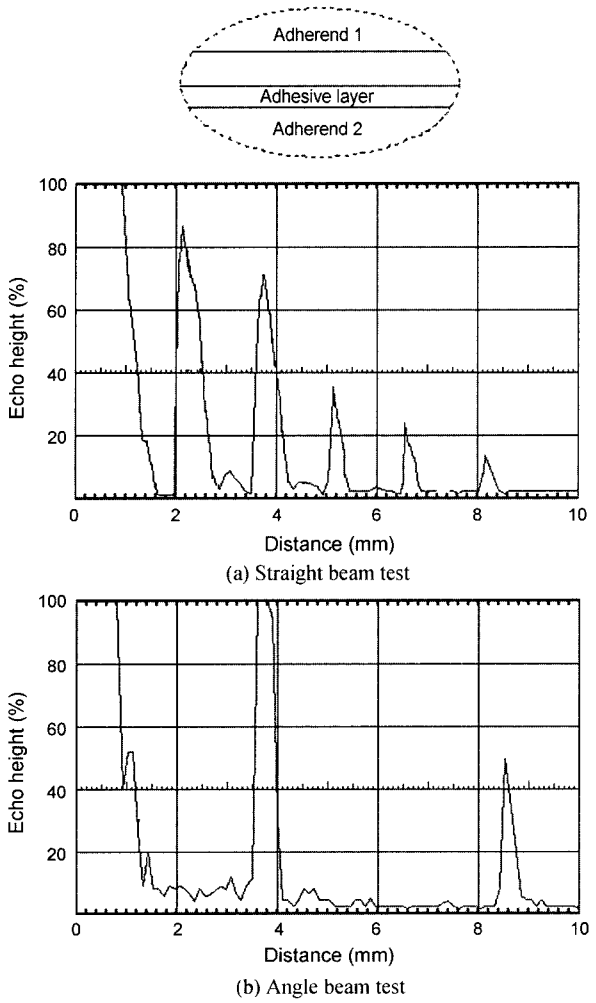

Figure 5. Ultrasonic test at position ① of Figure 4 in case of without crack.

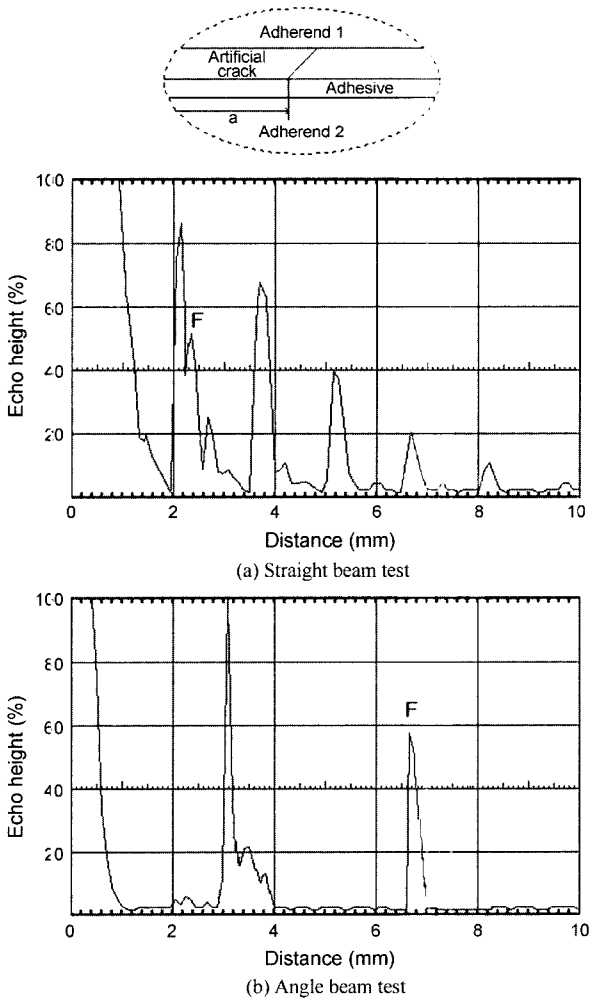

Figure 6. Echo of crack detection at position ② of Figure 4 in case of artificial crack.

the adhesive layer and it reflected once. It is because of the difference in the sound impedance of each material. In case of the angle beam test as shown in Figure 6(b), because of the differences in sound velocity and impedance of adherend, it was found that the echo appeared owing to reflection of the artificial crack-tip in the adhesive layer from the incidence point which is 0.5-skip distance. In the Figure 6, the point F indicates the ultrasonic echo from the flaw.

Figure 7 shows the enlarged shape of crack-tip when the crack has propagated along the upper adhesive interface between adherend 1 and adhesive as shown at position ③ of Figure 4.

As a load is applied to the specimen, the propagating crack-tip naturally shows a thumb-nail shape. Figure 7(a) shows the measured crack length by the straight beam test. The difference of crack length which was measured at crack-tip and crack side, indicates Δa. It was found that the ultrasonic echo of flaw was measured the crack-tip at center line on the width of specimen.

Figure 8 shows the enlarged shape of crack-tip when the crack has propagated along the lower adhesive interface between adherend 1 and adhesive as shown at position ④ of Figure 4. In case of the straight beam test as shown in Figure 8(a), the intensity of ultrasonic echo gradually decreases because adhesive layer exists on the crack and crack width near to crack-tip decreases.

The difference of crack length measured from the crack-tip to crack side, indicates Δa. In case of the straight beam test as sown in Figure 8(b), since the directions propagated by the echo and crack are not perpendicular, it is obvious that the intensity of echo decreases gradually. Comparing the echoes in Figure 7 and 8, the difference of echo generates in the direction of sound because the reflecting area at the crack-tip is small. In order to decrease the measuring error on crack-tip, its

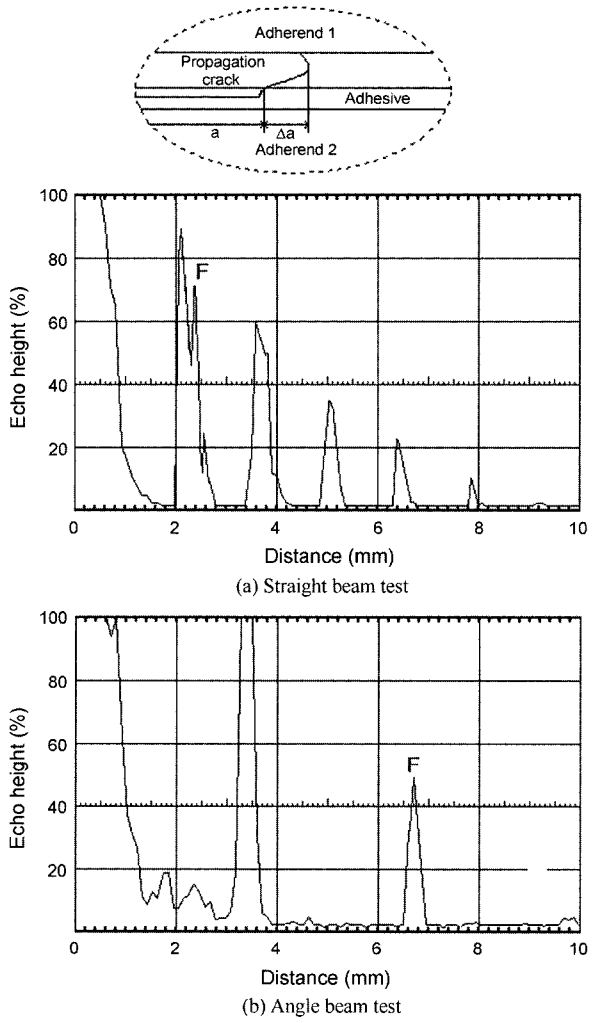

Figure 7. Echo of crack detection at position ③ of Figure 4 by ultrasonic test.

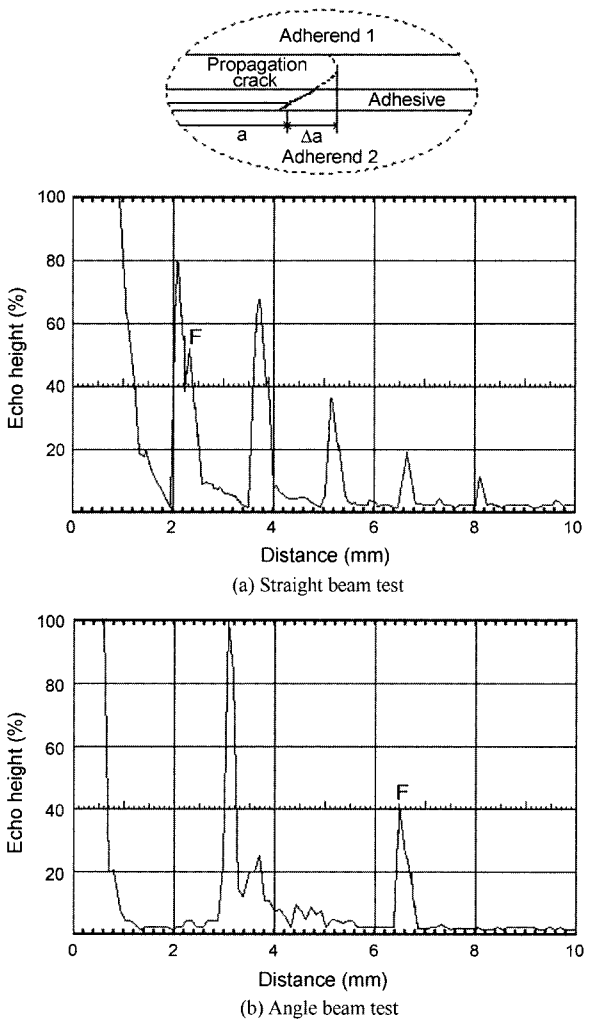

Figure 8. Echo of crack detection at position ④ of Figure 4 by ultrasonic test.

ultrasonic echo was compared with the trembler diameters of 5 mm and 10 mm in probes and the frequencies of 4 MHz and 5 MHz. If the trembler diameter of probe is smaller than the width of crack-tip or the frequency increases, the scatter of the beam decreases, and the sensitivity and resolution increases.

As shown in Figure 8(a), when the interfacial crack length increases with increasing the applied load, comparing the difference of crack length (Δa) for the side crack and central crack of specimen width, the difference indicates approximately 5%. The difference between the results of the measurement by the ultrasonic detection and by visual observation with a microscope was compared and estimated. Comparing the measured results by the ultrasonic detection and the observation of traveling microscope for the artificial crack-tip, the difference was approximately 3%.

4. PREDICTION OF INTERFACIAL CRACK LENGTH

The model of DCB specimen was analyzed with 2-dimensional elastic BEM program using Kelvin's fundamental solution. The model is divided into two areas for the adherends and one area for the adhesive ayer, and the total numbers of nods are 326.

The compliance for each crack length, a (mm), can be obtained from the following equation.

$$C=\frac{\delta}{P}(mm/N) \tag{3}$$

where $P(N)$ is the applying load and δ (mm) is displacement at loading point.

Substituting the displacement of load point obtained by BEM analysis for the crack length into equation (3),

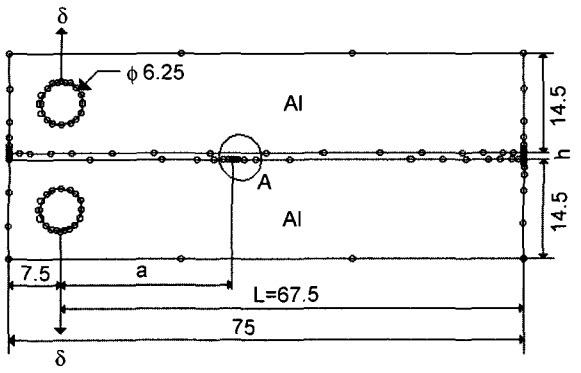

Figure 9. Typical mesh pattern of BEM model.

the compliances are plotted as shown in Figure 10.

As the crack length gets longer the change of compliance also increases non-linearly. On the other hand, Ripling's equation is an approximate equation to estimate the compliance of DCB specimen of the homogeneous materials without the adhesive layer. Then, Ripling's equation is given as follows (Ripling, 1964):

$$C=\frac{1}{3EI}[(a+a_0)^3+H^2a] \tag{4}$$

where E is Young's modulus of adherend, H is specimen height, I is moment of inertia, a_o is rotation of the beam at crack-tip, and H^2a is the shear modification.

Variation of the compliance for the crack length, which was analyzed by BEM and Ripling's equation, was shown in Figure 10. The variation of compliances shows increasing tendency according to increase of the crack length. The results (Chung, 2000) by BEM are slightly higher than those obtained by Ripling's equation. It is considered that the thickness, visco-elasticity and plasticity for used adhesive affect the difference in compliances.

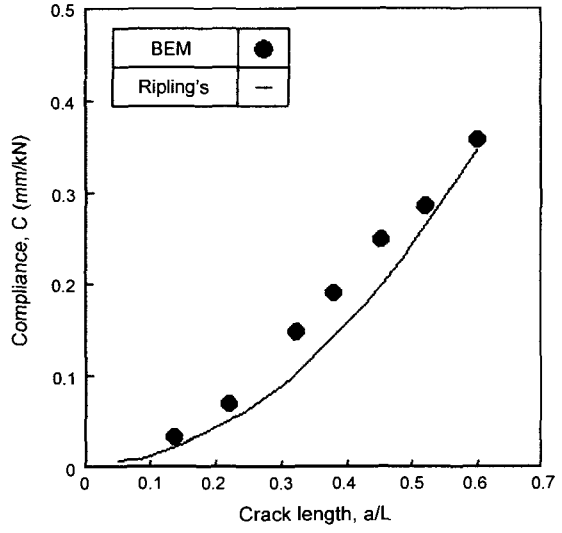

Figure 10. Comparison of BEM analysis and Riplings equation.

5. RESULTS AND DISCUSSION

The variation of experimental compliance versus crack length was plotted in Figure 11.

It shows experimental results from the straight and angle beam test for the thickness of adhesive layer, h=0.2 mm. 2 mm. In Figure 11, the difference of compliances which is obtained from the straight and angle beam tests with the thickness of adhesive layer, h=0.2 mm, 2 mm, is so small that it can be ignored.

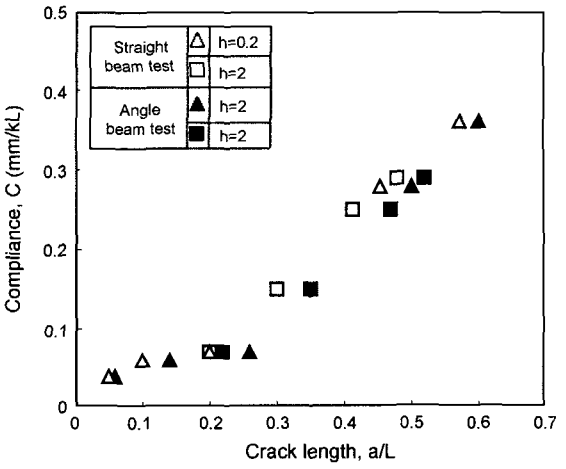

Figure 11. Relation between compliance and crack length by ultrasonic test.

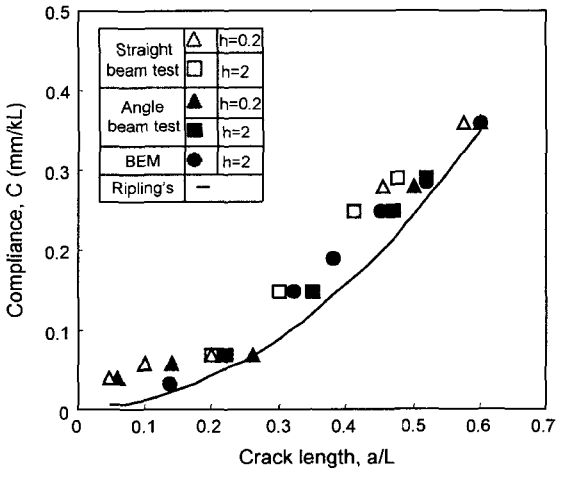

Figure 12. Comparison of accuracies by BEM analysis, Replings equation and ultrasonic test.

Figure 12 shows negligible the difference between interfacial crack lengths obtained by three different methods, ultrasonic, BEM analysis, and Ripling's equation.

Considering the difference of crack length measured by each method, the values obtained by the ultrasonic method are in good agreement with the computed results by BEM. And also, comparing with the interfacial crack lengths calculated from Ripling's equation, the values are corresponded within 5% error.

The difference is explained by the fact that the effects of thin adhesive layer, material properties, measuring error of crack length and overlap of sound are mutually correlated. Considering these comparative analyses, ultrasonic method is very useful to detect the interface cracks in adhesively bonded joints and structures.

6. CONCLUSIONS

The ultrasonic method to detect interface crack was applied to the adhesively bonded joints of double-cantilever beam. The optimal condition of transmission coefficients and experimental accuracy on interface crack by ultrasonic method were investigated. The results obtained are summarized as follows:

(1) The experimental values of interfacial crack length using the ultrasonic method are in good agreement with the computed result by BEM, and comparing with the result of Ripling's equation the values are corresponded within 5% error.

(2) In the case of the straight beam test, we made a new layer using the Cemedine 1500, which indicates the identical velocity of ultrasonic wave for the adhesive. The detecting and resolving abilities of flaws are greatly improved by the increase of sound pressure within the range of $\lambda/3<h<2\lambda$.

(3) When the difference between the ultrasonic velocities of adherends and adhesive in the adhesively of bonded DCB joints is greater than 1.5~2, the accuracy resolving power and the detecting ability of crack are reduced due to the difference of sound impedance.

(4) In case of the angle beam test, the optimal test condition can be obtained within the range of incidence angle, 20°~30° and 60°~80°.

REFERENCES

Adler, L. and Whaley, H. L. (1972). Interference effect in a multifrequency ultrasonic pulse echo and its application to flaw characterization. *Journal of Acoustical Society of America*, **51**, **3**, 76–84.

Chung, N. Y., Kang, S. K. and Lee, M. D. (2000). Analyses of stress intensity factors and evaluation of fracture toughness in adhesively bonded DCB joints. *KSME*, **24**, **6**, 1547–1556.

Chung, N. Y., Park, S. I. and Lee, M. D. (2001). Detection of interface crack using ultrasonic method in adhesively bonded joints. *KSME*, **25**, **3**, 566–572.

Derouiche, Z. and Dlebarre, C. (1995). Ultrasonic characterization of heterogeneous materials using a stochastic approach. *J. Acoust. Soc. Am.*, **97**, **4**, 2304–2315.

Kline, R. A., Hsiao, C. P. and Fidaali, M. A. (1986). Nondestructive evaluation of adhesively bonded joint. *Trans. ASME*, July, 214–217.

Kline, R. A. and Hashemi, D. (1987). Ultrasonic guide-wave monitoring of fatigue damage development in bonded joint. *ASNT*, Sep., 1076–1082.

Koike, T. (1990). Analysis of ultrasonic received power using K-scan technique for dovetail inspection of turbine disks. *JSME*, **41**, **4**, 207–214.

Moriyama, K. (1998). Effect of surface roughness on sensitivity of ultrasonic normal beam test. *JSNDI*, **47**, **5**, 315–321.

Ripling, E. J., Mostovoy, S. and Patrick, R. L. (1964). Measuring fracture toughness of adhesive joints. *Materials Research Standard*, **4**, 129–134.